16th World Conference on Earthquake Engineering, 16WCEE 2017
Santiago Chile, January 9th to 13th 2017
Paper N°_3829
Registration Code: S-J1463692100

DESIGN OF STEEL-PLATE CONCRETE COMPOSITE WALL PIERS

S. Epackachi [1], A.S. Whittaker [2]

[1] Teaching Assistant Professor, Dept. of Civil, Structural and Environmental Engineering, University at Buffalo, Buffalo, NY 14260. Email: siamakep@buffalo.edu

[2] Professor; Director, MCEER; Dept. of Civil, Structural and Environmental Engineering, University at Buffalo, Buffalo, NY 14260. Email: awhittak@buffalo.edu

Abstract

The lack of analysis, design and detailing guidance in standards and manuals has contributed to the limited use of steel-plate concrete (SC) composite shear walls. In this paper, a process to design SC wall piers is proposed, which accounts for wall aspect ratio, faceplate reinforcement ratio, axial force, and concrete and faceplate strengths. The mechanics-based equations are used to generate axial force-bending moment interaction curves for different material properties and aspect ratios. The proposed design equations may be suitable for inclusion in a seismic design standard.

Keywords: composite shear wall; mechanics-based equations; interaction curve; parametric analysis; design guideline.

1. Introduction

A steel-plate concrete (SC) composite shear wall is a plain concrete wall with two thin steel faceplates. Headed studs are used to anchor the steel faceplates to the infill concrete and tie rods are used to join the steel faceplates. The connectors (i.e., headed studs and tie rods) are attached to the steel faceplates by welded or bolted connections. The faceplates provide both formwork and reinforcement.

The use of SC walls in nuclear power plants in Korea, Japan, and the United States has been studied for nearly 30 years, with an emphasis on elastic response in design basis shaking [1, 2, 3, 4, 5, 6, 7, 8]. SC walls have not been used for earthquake-resistant building construction, in part due to lack of reliable information for their analysis and design. The recently issued AISC N690-12 Supplement 1 [9] includes specifications for the design of labyrinthine SC walls (i.e., interconnected SC walls that are assumed to be shear-critical in plane) that used inside containment in nuclear power plants. The draft Standard AISC 341-16 [10] includes provisions for design of composite plate shear walls-concrete filled (C-PSW/CF) with and without boundary elements. AISC 341-16 estimates the strength of a wall by a yield moment that corresponds to the onset of steel faceplate yielding at its compression toe. The yield moment is calculated assuming a linear elastic stress distribution with maximum concrete compressive stress equal to $0.7f_c'$ and maximum steel stress equal to f_y. This simplified proposed method does not address co-existing shear and axial forces.

Herein, the results of a comprehensive parametric study are used to derive a design-oriented predictive equation for peak lateral strength of SC wall piers without boundary elements. The interaction between shear force, axial force and bending moment is considered and wall aspect ratio, reinforcement ratio, axial load, and steel and concrete strengths are addressed. The proposed equations are used to generate axial force-bending moment (P-M) interaction curves that could facilitate the design of SC walls.

2. Basis for design of SC walls

The in-plane seismic response of an SC wall pier is affected by its aspect ratio, the faceplate reinforcement ratio, the faceplate slenderness ratio, the yield strength of the steel faceplates, the uniaxial compressive strength of the infill concrete and the co-existing axial load. These effects have been characterized recently [11, 12] in a detailed

parametric study using the general purpose finite element code, LS-DYNA [13, 14]. The baseline LS-DYNA model was validated using the local and global nonlinear cyclic in-plane responses of SC wall piers tested at the University at Buffalo [15, 16].

The results of the parametric study were used to develop a mechanics-based equation for peak lateral strength and regression-based predictive equations to establish tri-linear lateral force-displacement relationship up to peak strength. Both sets of equations address the interaction of co-existing shear and axial force, and bending moment and could be implemented in seismic design standards. The derivations of the predictive equations are provided in Epackachi et al. [12] and are not repeated here.

2.1. Numerical modeling assumptions

The LS-DYNA model used for the parametric study is described in Fig. 1. The infill concrete and the steel faceplates were modeled using the Winfrith concrete model, MAT085, and Piecewise-Linear-Plasticity model, MAT024, respectively. The Winfrith concrete model, developed by Broadhouse [17], is a smeared crack model; its yield surface is based on the four-parameter plastic surface of Ottosen model [18]. Tension stiffening is considered using either linear or bilinear post-cracked tensile response. Eight-node ($1\times1\times1$ in.) solid elements with a constant stress formulation [14] and 1×1 in. four-node shell elements with Belytschko-Tsay formulation [14] were used to model the infill concrete and steel faceplates, respectively.

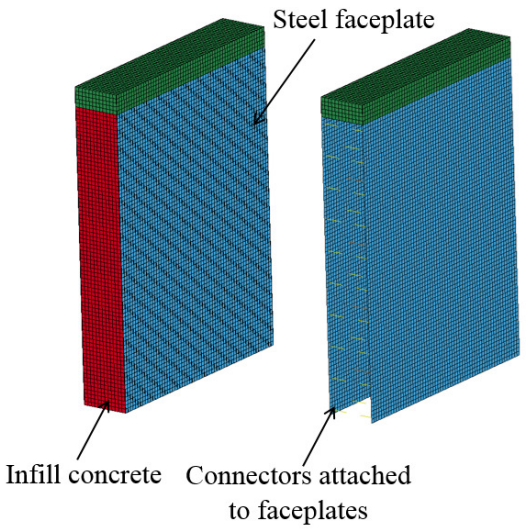

Fig. 1 – LS-DYNA model [12]

The length and thickness of the walls were set to 60 in. and 12 in., respectively. A fixed-base was assumed. Composite action was considered using a coefficient of friction between the steel faceplates and infill concrete equal to 0.57, based on the test results presented in Rabbat et al. [19]. The chosen stud spacing prevented elastic local buckling of the steel faceplates. Tie rods were spaced at a distance equal to the wall thickness. Beam elements were used to model the connectors and were fully tied to the solid concrete elements.

2.2. Parametric study of SC walls

The parametric study addressed a wide range of design variables: wall aspect ratio ranging from 0.3 to 3.0, faceplate reinforcement ratio ranging from 1% to 9%, axial load ratio ranging from 0 to 0.2, yield strength of the steel faceplates between 34 and 67 ksi, and concrete compressive strength between 4 and 8 ksi. The reinforcement ratio is defined as the ratio of the cross-sectional area of the steel faceplates to the total cross-sectional area of SC

wall. The axial load ratio is the applied axial compressive force divided by the product of the concrete compressive strength and the total cross-sectional area of the SC wall.

The results of the parametric study were used 1) to develop a mechanics-based equation for peak lateral capacity of SC wall piers, and 2) as input data for statistical analyses investigating the main and interaction effects of design variables on the lateral load capacity and stiffness of SC wall piers [12].

2.3. Mechanics-based predictive equation for lateral load capacity

The predictive equation for the peak lateral capacity of an SC wall pier was formulated using the results of the parametric study, including the distribution of vertical stress in the steel faceplates and the infill concrete along the length of the wall at peak lateral load. In this study, SC walls with an aspect ratio of 1.5 and less are denoted as "low-aspect ratio" and the walls with an aspect ratio of greater than 1.5 are denoted as "high-aspect ratio". The results of the parametric study indicated that 1) the vertical stress distribution in the steel faceplates is significantly affected by wall aspect ratio, reinforcement ratio, and axial load and it can be represented by a bilinear relationship for low-aspect ratio walls and by a linear relationship for high-aspect ratio walls; 2) the neutral axes of the infill concrete and steel faceplates do not coincide in low-aspect ratio SC walls due to shear-flexure interaction: the difference between the neutral axis depth of the infill concrete and steel faceplates reduces as the wall aspect ratio increases; 3) the maximum strain at the compression toe of the wall is a function of aspect ratio and it varies from the yield strain of the steel faceplates to the ultimate concrete strain as the wall aspect ratio increases from 0.3 to 3; 4) as aspect ratio increases, the maximum vertical strain at the base of the wall increases resulting that the maximum vertical steel stress exceeds from the yield stress due to hardening and tensile stress of concrete decreases due to cracking. These effects were considered in the derivation of the mechanics-based equation.

Three strength factors, λ_1, λ_2, and λ_3, were included in the formulation to consider 1) the effect of aspect ratio on the maximum strain at the compression toe of the wall, 2) the effect of aspect ratio on difference between the neutral axis depths of the infill concrete and steel faceplates, and 3) the effects of aspect ratio, reinforcement ratio, and axial load on the vertical stress distribution in the steel faceplates on the tension side for low-aspect ratio SC walls, respectively. The distributions of vertical strain and stress in the steel faceplates and infill concrete are presented in Fig. 2.

In Fig. 2, t_c and t_s are the thicknesses of the infill concrete and steel faceplates, respectively, L is the length of the wall, c and c' are the depths to the neutral axes of the steel faceplates and infill concrete from compression end of the wall, respectively, f_s^* and f_t^* are the maximum vertical steel stress and the modified tensile stress of concrete, respectively, ε_c is the maximum compressive strain varying from the yield strain of the steel faceplates, ε_y, to the concrete strain corresponding to the peak stress, ε_{cu} (=0.004), and β_1 and β_2 are the stress block parameters.

3. A design procedure for SC wall piers

A design procedure for an SC wall pier without boundary elements includes the following steps, which are easily coded: the mechanics-based design equation identified previously. Not included here are strength reduction factors (ϕ in US practice), which would be specified by a standards committee.

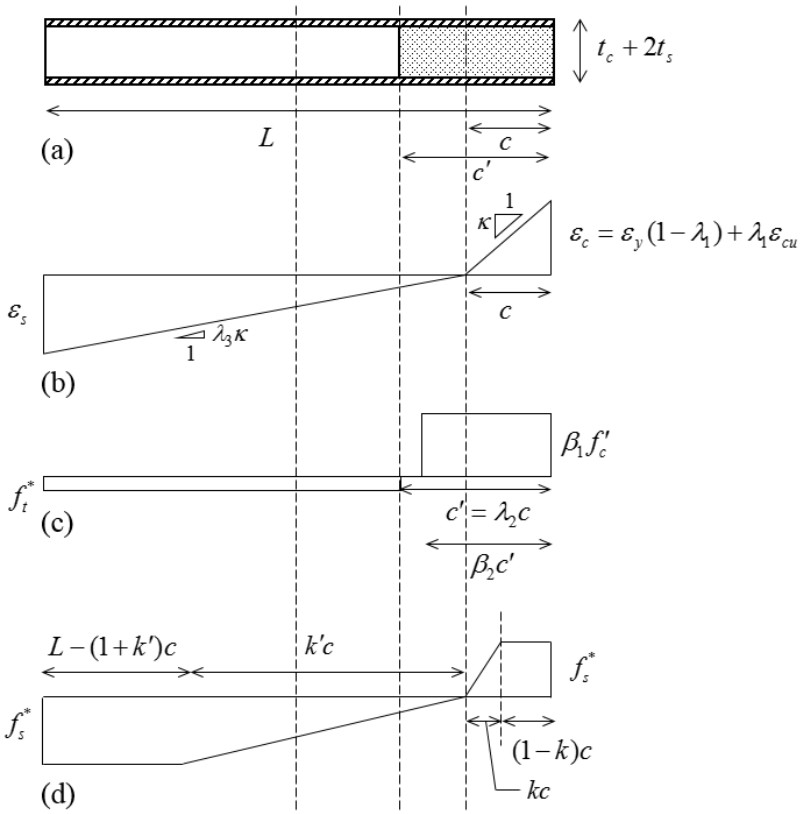

Fig. 2 – Moment capacity calculation; (a) SC wall cross section; (b) vertical strain profile; (c) vertical profile in infill concrete; and (d) vertical stress profile in steel faceplates [12]

Step 1: Calculate the demands on the critical cross-section of SC wall. As an example, Fig. 3 presents a schematic drawing of an SC wall subjected to three factored lateral loads (F_1 to F_3) and three factored axial loads (N_1 to N_3). The factored axial and shear forces, and bending moment applied on the critical cross-section, at the base of the wall, are calculated as:

$$P_u = N_1 + N_2 + N_3 \tag{1}$$

$$V_u = F_1 + F_2 + F_3 \tag{2}$$

$$M_u = F_3(h_1 + h_2 + h_3) + F_2(h_1 + h_2) + F_1(h_1) \tag{3}$$

Step 2: Assume a concrete compressive stress, f'_c, concrete tensile stress, f_t, and steel yield stress, f_y.

Step 3: Assume an infill concrete thickness, t_c, within the range of $0.1L$ to $0.2L$.

Step 4: Calculate the normalized moment-to-shear ratio, M/VL, using the values of the shear force and bending moment, calculated in step 1. Note that the normalized moment-to-shear ratio is identical to the wall aspect ratio for a single story wall panel (i.e., a wall panel subjected to a lateral load at top of the wall).

Step 5: Assume a reinforcement ratio, ρ_s, within the range of 1% to 9%.

Step 6: Calculate the steel faceplate thickness, t_s:

$$t_s = \frac{\rho_s t_c}{2(1-\rho_s)} \tag{4}$$

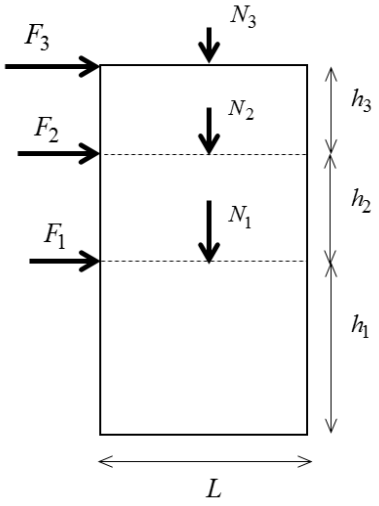

Fig. 3 – SC wall pier subjected to lateral and axial loads

Step 7: Calculate the maximum vertical stress of the steel faceplates, f_s^*, and the modified tensile stress in the infill concrete, f_t^*, corresponding to the peak lateral strength of SC wall:

$$1.05 f_y \le f_s^* = \left[1.05 + 0.056(M/VL - 0.3)\right] f_y \le 1.2 f_y \tag{5}$$

$$0 \le f_t^* = 0.185(3 - M/VL) f \le 0.5 f_t \tag{6}$$

Step 8: Calculate the strength modification factors λ_1, λ_2, and λ_3. If the ratio of M/VL, calculated in step 4, is greater than or equal to 1.5, then $\lambda_1 = \lambda_2 = \lambda_3 = 1.0$, otherwise, the factors λ_1, λ_2, and λ_3 are:

$$\lambda_1 = \frac{M/VL - 0.3}{1.2} \tag{7}$$

$$\lambda_2 = 1.42(M/VL)^{-0.86} \tag{8}$$

$$\lambda_3 = (1 + \frac{P_u}{0.2 f_c' A_g}(1.21(M/VL)^{-0.48} - 1))(0.05\exp(2M/VL))(0.17\rho_s + 0.75) \le 1.0 \tag{9}$$

where A_g is the total cross-sectional area of the wall (i.e., $(2t_s + t_c)L$).

Step 9: Calculate the maximum compressive strain, ε_c, as:

$$\varepsilon_c = \varepsilon_y(1 - \lambda_1) + \varepsilon_{cu}\lambda_1 \tag{10}$$

where ε_y is the yield strain of the steel faceplates, and ε_{cu} is the concrete strain corresponding to the peak stress (=0.004).

Step 10: Calculate the stress block parameters, β_1 and β_2, as a function of ε_c, using Table 1.

Step 11: Calculate the parameters φ, φ', and k :

$$\varphi = \frac{\beta_1 \beta_2 f_c'}{\rho_s f_s^*} \tag{11}$$

$$\varphi' = \frac{f_t^*}{\rho_s f_s^*} \tag{12}$$

$$k = \frac{\varepsilon_y}{\varepsilon_c} \tag{13}$$

Table 1 – Values of the stress block parameters

ε_c	β_1	β_2
0.001	0.55	0.70
0.0015	0.75	0.72
0.002	0.88	0.75
0.0025	0.94	0.78
0.003	0.96	0.81
0.0035	0.97	0.83
0.004	0.98	0.85

Step 12: Calculate the depth to the neutral axis from the compression toe, c :

$$c = \frac{\frac{P_u}{A_s f_y} + 1 + \varphi'}{\lambda_2(\varphi + \varphi') + k(1-\lambda_3)/(2\lambda_3) + 2} \tag{14}$$

Step 13: Calculate the minimum value of the strength modification factor λ_3 :

$$\lambda_{3\min} = \frac{\varepsilon_y \alpha}{(1-\alpha)\varepsilon_c} \tag{15}$$

where α is the normalized neutral axis depth (i.e., $\alpha = c/L$). If the factor λ_3 calculated in step 8 is less than $\lambda_{3\min}$, return to step 12 and recalculate the depth to the neutral axis assuming $\lambda_3 = \lambda_{3\min}$.

Step 14: Calculate L_c , L_c' , and L_s as:

$$L_c = L\left[\lambda_2 \alpha (1 - \beta_2 \lambda_2 \alpha)/2\right] \tag{16}$$

$$L_c' = L\left[\lambda_2 \alpha (1 - \lambda_2 \alpha)/2\right] \tag{17}$$

$$L_s = \alpha L\left[1 + 0.25k(1/\lambda_3 - 1) - \alpha(1 + 0.5k(1/\lambda_3 - 1) + k^2(1/\lambda_3{}^2 + 1)/6)\right] \tag{18}$$

Step 15: Calculate the nominal bending moment capacity of the SC wall cross-section as:

$$M_n = \beta_1 \beta_2 f_c' A_c L_c + A_s f_s^* L_s + A_c f_t^* L_c' \tag{19}$$

where A_c is the cross-sectional area of the infill concrete ($= t_c L$), and A_s is the cross-sectional area of the steel faceplates ($= 2t_s L$).

Step 16: Check the ratio of M_u / M_n , noting that the strength modification factor was taken as 1.0. If the ratio is less than 1, the design is satisfactory. If the ratio is greater than 1, the design is unconservative and redesign is needed (i.e., higher material strengths, greater material thickness).

Step 17: Calculate the spacing and diameter of connectors using the specifications of Section 7.4 of AISC 341-16 [10].

4. Design of SC wall piers using P-M interaction curves

4.1 Using the interaction curves

To facilitate the design of SC wall piers, 27 axial force-bending moment interaction diagrams are generated for concrete compressive strengths of 4, 6, and 8 ksi, steel yield strengths of 34, 50, and 67 ksi, and aspect ratios of 0.5, 1, and 2. The *P-M* interaction diagrams are presented in Fig. 5 (Appendix A). Not included here are strength reduction factors, which would be specified by a standards committee. The diagrams can be used as follows.

Steps 1 to 6: See steps 1 to 6 presented in Section 3 of this paper.

Step 7: Identify the interaction diagram in Appendix A that best maps to the user-selected values of f_c', f_y, and aspect ratio (or moment-to-shear ratio for a wall subjected to multilateral loads).

Step 8: Plot the coordinates (M_u / M_*, P_u / P_*) on the chosen interaction curve, where P_* and M_* are the plastic capacities of the cross-section:

$$P_* = A_c f_c' + A_s f_y \tag{20}$$

$$M_* = 0.72 f_c' A_c L_c + A_s f_y L_s \tag{21}$$

where L_c and L_s are calculated as:

$$L_c = \alpha L\left(\frac{1-0.85\alpha}{2}\right) \tag{22}$$

$$L_s = \alpha L(1-1.5\alpha) \tag{23}$$

where α is calculated as:

$$\alpha = \frac{1}{\frac{0.72 A_c f_c'}{A_s f_y} + 2} \tag{24}$$

The strain and stress profiles used in the derivation of plastic moment capacity are presented in Fig. 4.

Step 9: Check the step 5 assumption regarding reinforcement ratio and iterate for a design solution.

Step 10: Calculate the spacing and diameter of connectors using Section 7.4 of AISC 341-16 [10].

4.2 A design example

To illustrate the use of the interaction charts, consider the three-story wall of Fig. 3, with (F_1, F_2 and F_3) equal to (300, 400, and 500 kips), (N_1, N_2 and N_3) equal to (250, 250, and 200 kips), and (h_1, h_2 and h_3) equal to (15, 12, and 12 feet). Assume *L* equal to 25 feet, a wall thickness of 8 inches, a reinforcement ratio of 3% leading to a steel faceplate thickness of 0.12 inches per Eq. (9), a uniaxial concrete compressive strength of 4 ksi, and steel faceplate yield strength of 50 ksi. Forces V_u, P_u and M_u at the base of the wall are 1200 kips, 700 kips, and 34800 kip-ft, respectively. The moment-to-shear ratio at the base of the wall, normalized by the length of the wall, is 1.20. Using the interaction charts in Fig. 5 corresponding to $f_c' = 4$ ksi and $f_y = 50$ ksi, and aspect ratios of 1.0 and 2.0, and noting that $P_* = 13310$ kips and $M_* = 32140$ kips-ft, and thus $P_u / P_* = 0.05$ and $M_u / M_* = 1.08$, the required reinforcement ratio (RR) is 1% for both aspect ratios of 1.0 and 2.0: much different from the assumed value of 3%. The design coordinate (0.05, 1.08) is shown as a red solid circle on these interaction charts in Fig. 5. The design could terminate here, with a reinforcement ratio of 3%.

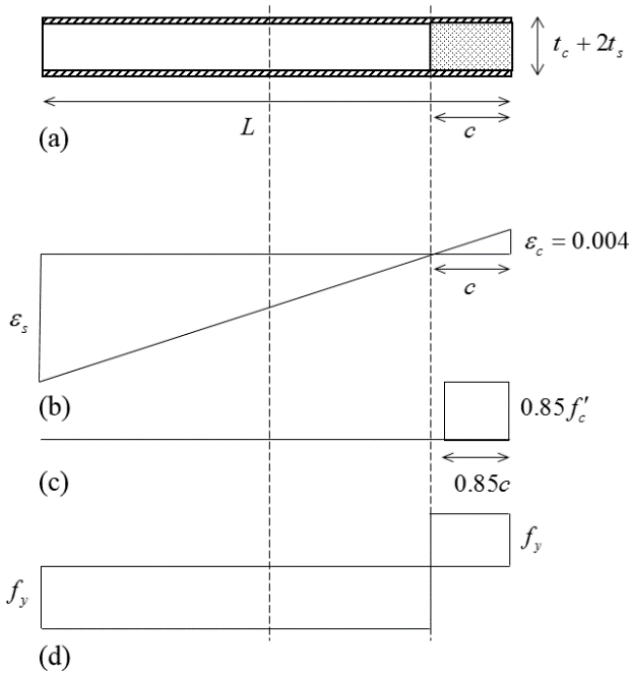

Fig. 4 – Plastic moment capacity calculation; (a) SC wall cross section; (b) vertical strain distribution; (c) vertical stress distribution in infill concrete; and (d) vertical stress distribution in steel faceplates [12]

For the next iteration, assume now a RR of 2%, which leads to the design coordinate of (0.06, 1.48) that is shown as the open red circle on these interaction charts. As seen in Fig. 5, the open red circles fall outside the interaction curves corresponding to 2% reinforcement ratio for both aspect ratios of 1.0 and 2.0 meaning that the design is unconservative. So, the required reinforcement ratio and the corresponding steel faceplate thickness are 3% and 0.12 inch, respectively. Assuming a yield stress of 50 ksi for connectors, the corresponding maximum spacing and diameter of the connectors are 3 in. and 0.25 in. per Section 7.4 of AISC 341-16. (Because the cost of installing the studs and connectors may exceed the cost of the faceplate, the most economical solution may involve increasing the faceplate thickness (and thus increasing capacity) and increasing the stud spacing, but economy is not the subject of this paper.)

5. Conclusion

The results of a comprehensive parametric study have been used to derive design equations for the peak lateral resistance of SC wall piers. The effects of wall aspect ratio, reinforcement ratio, axial load, yield strength of the steel faceplates, and uniaxial compressive strength of concrete are considered explicitly. Numerical analysis showed that the distribution of the vertical stress in the steel faceplates and the infill concrete are significantly affected by aspect ratio. The response is also affected by shear and axial force interaction, suggesting that simplified methods that ignore this interaction cannot reliably predict the lateral load capacity of an SC wall. The mechanics-based equation derived herein addresses the interaction of co-existing shear and axial force.

Design recommendations were provided for SC walls including expressions to calculate the required wall dimensions to resist the applied axial and lateral loads. These mechanics-based equations were used to generate a series of axial force-bending moment interaction curves that could serve as a design aid for determining the required thickness of the steel faceplates. Not included to date are strength reduction factors, which should be specified by a standards committee. A design example was presented to illustrate the calculation procedure.

6. References

[1] Akiyama H, Sekimoto H, Tanaka M, Inoue K, Fukihara M, Okuda Y (1989): 1/10th scale model test of inner concrete structure composed of concrete filled steel bearing wall. *10th International Conference on Structural Mechanics in Reactor Technology (SMiRT10),* International Association for Structural Mechanics in Reactor Technology (IASMiRT), Anaheim, California, USA.

[2] Sasaki N, Akiyama, H, Narikawa M, Hara K, Takeuchi M, Usami S (1995): Study on a concrete filled steel structure for nuclear power plants (part #2): shear and bending loading tests on wall member. *13th International Conference on Structural Mechanics in Reactor Technology (SMiRT13),* International Association for Structural Mechanics in Reactor Technology (IASMiRT), Porto Alegre, Brazil.

[3] Takeda T, Yamaguchi T, Nakayama T, Akiyama K, Kato Y (1995): Experimental study on shear characteristics of concrete filled steel plate wall. *13th International Conference on Structural Mechanics in Reactor Technology (SMiRT13),* International Association for Structural Mechanics in Reactor Technology (IASMiRT), Porto Alegre, Brazil.

[4] Ozaki M, Akita S, Osuga H, Nakayama T, Adachi N (2004): Study on steel plate reinforced concrete panels subjected to cyclic in-plane shear. *Nuclear Engineering and Design*, **228**(1-3), 225-244.

[5] Eom TS, Park HG, Lee CH, Kim JH, Chang IH (2009): Behavior of double skin composite wall subjected to in-plane cyclic loading. *Journal of Structural Engineering*, **135**(10), 1239-1249.

[6] Jian-Guo N, Hong-Song H, Jian-Sheng F, Mu-Xuan T, Sheng-Yong L, Fu-Jun L (2013): Experimental study on seismic behavior of high-strength concrete filled double-steel-plate composite walls. *Journal of Constructional Steel Research*, **88**, 206-219.

[7] Nie JG, Ma XW, Tao MX, Fan JS, Bu FM (2014): Effective stiffness of composite shear wall with double plates and filled concrete. *Journal of Constructional Steel Research*, **99**, 140-148.

[8] Varma AH, Malushte SR, Sener KC, Lai Z (2014): Steel-plate composite (SC) walls for safety-related nuclear facilities: Design for in-plane forces and out-of-plane moments. *Nuclear Engineering and Design*, **269**(1), 240-249.

[9] American Institute of Steel Construction (2014): Specification for safety-related steel structures for nuclear facilities, Supplement No. 1. N690s1, *American Institute of Steel Construction*, Chicago, IL.

[10] American Institute of Steel Construction (2016): Seismic provisions for structural steel buildings. *American Institute of Steel Construction*, Chicago, IL.

[11] Epackachi S, Whittaker AS (2016): Experimental, numerical, and analytical studies on the seismic response of steel-plate concrete (SC) composite shear walls. *Technical report MCEER 16-0001*, University at Buffalo, State University of New York, Buffalo, NY.

[12] Epackachi S, Whittaker AS, Aref AJ (2016): Seismic analysis and design of steel-plate concrete wall piers. *Engineering Structures*, Under Review.

[13] LS-DYNA (2012): Keyword User's Manual, Volume I. *Version 971 R6.0.0*, Livermore, CA, USA.

[14] LS-DYNA (2012): Keyword User's Manual, Volume II. *Version 971 R6.0.0*, Livermore, CA, USA.

[15] Epackachi S, Nguyen NH, Kurt EG, Whittaker AS, Varma AH (2013): In-plane seismic behavior of rectangular steel-plate composite wall piers. *Journal of Structural Engineering (ASCE)*, **141**(7), 1-9.

[16] Epackachi S, Whittaker AS, Varma AH, Kurt EG (2015): Finite element modeling of steel-plate concrete composite wall piers. *Engineering Structures*, **100**, 369-384.

[17] Broadhouse BJ (1986): DRASTIC-A compute code for dynamic analysis of stress transients in reinforced concrete. *Safety and Engineering Science Division*, AEE, Winfrith, AEEW – R2124.

[18] Ottosen NS (1977): A failure criterion for concrete. *Journal of the Engineering Mechanics Division*, **103**(4), 527-535.

[19] Rabbat BG, Russell HG (1985): Friction coefficient of steel on concrete or grout. *Journal of Structural Engineering*, **111**(3), 505-515.

Appendix A: P-M interaction curves for SC walls

The *P-M* interaction curves for uniaxial concrete compressive strength of 4, 6, and 8 ksi, steel yield strength of 34, 50, and 67 ksi, and wall aspect ratio of 0.5, 1, and 2, are presented in Fig. 5, where RR denotes reinforcement ratio. The interaction charts were generated using the coordinates (M_n / M_*, P_n / P_*), where P_n is the axial force at $M_n = 0$. Note that M_n at zero axial load can exceed M_* because the steel and concrete stress distributions used to calculate M_n (see Fig. 2), are different from those used for M_* as presented in Fig. 4. Similarly, the axial force P_n calculated using Eqs. 9 to 19 does not equal P_* defined per Eq. 20.

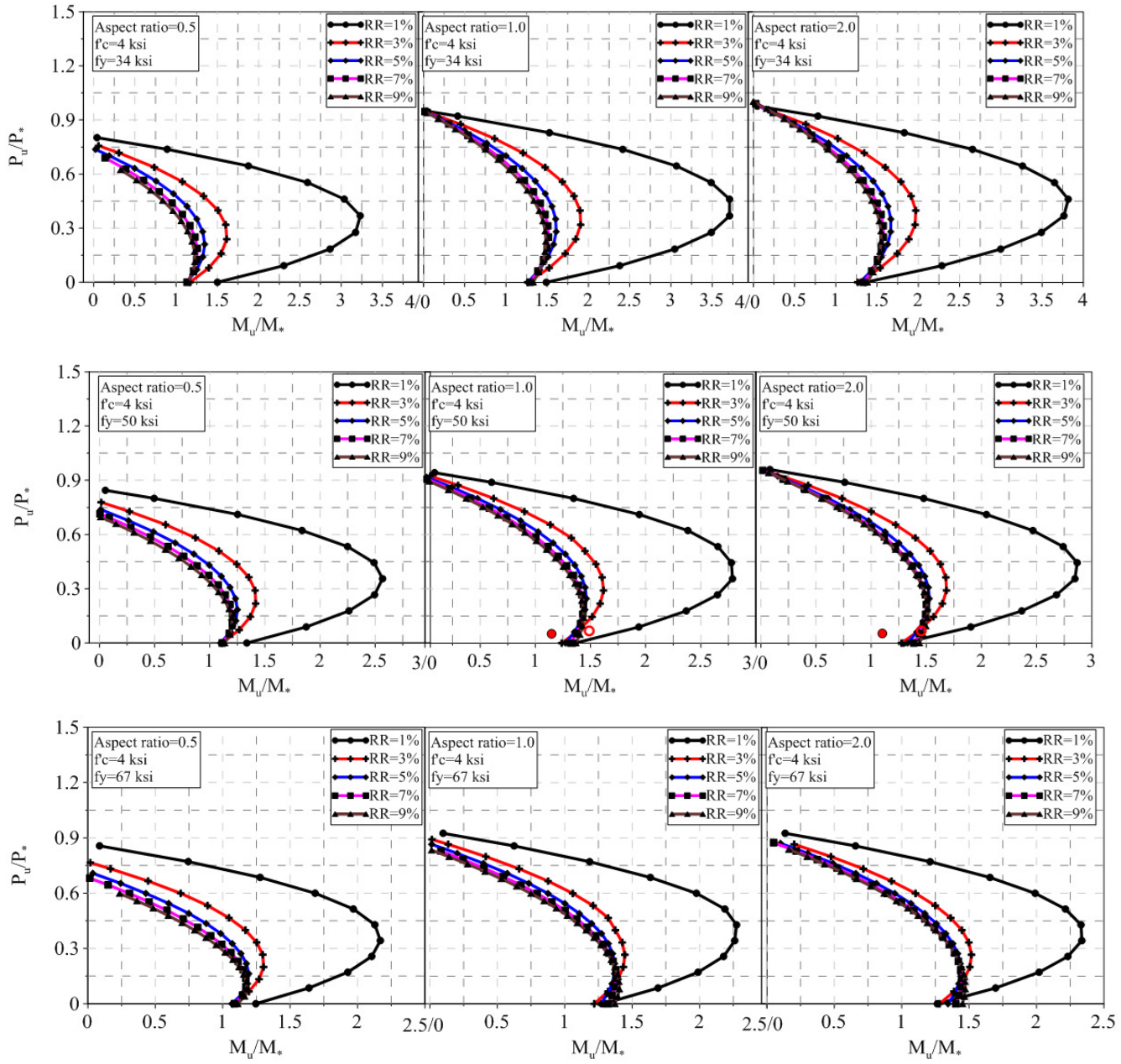

Fig. 5 – P-M interaction curves for SC wall piers

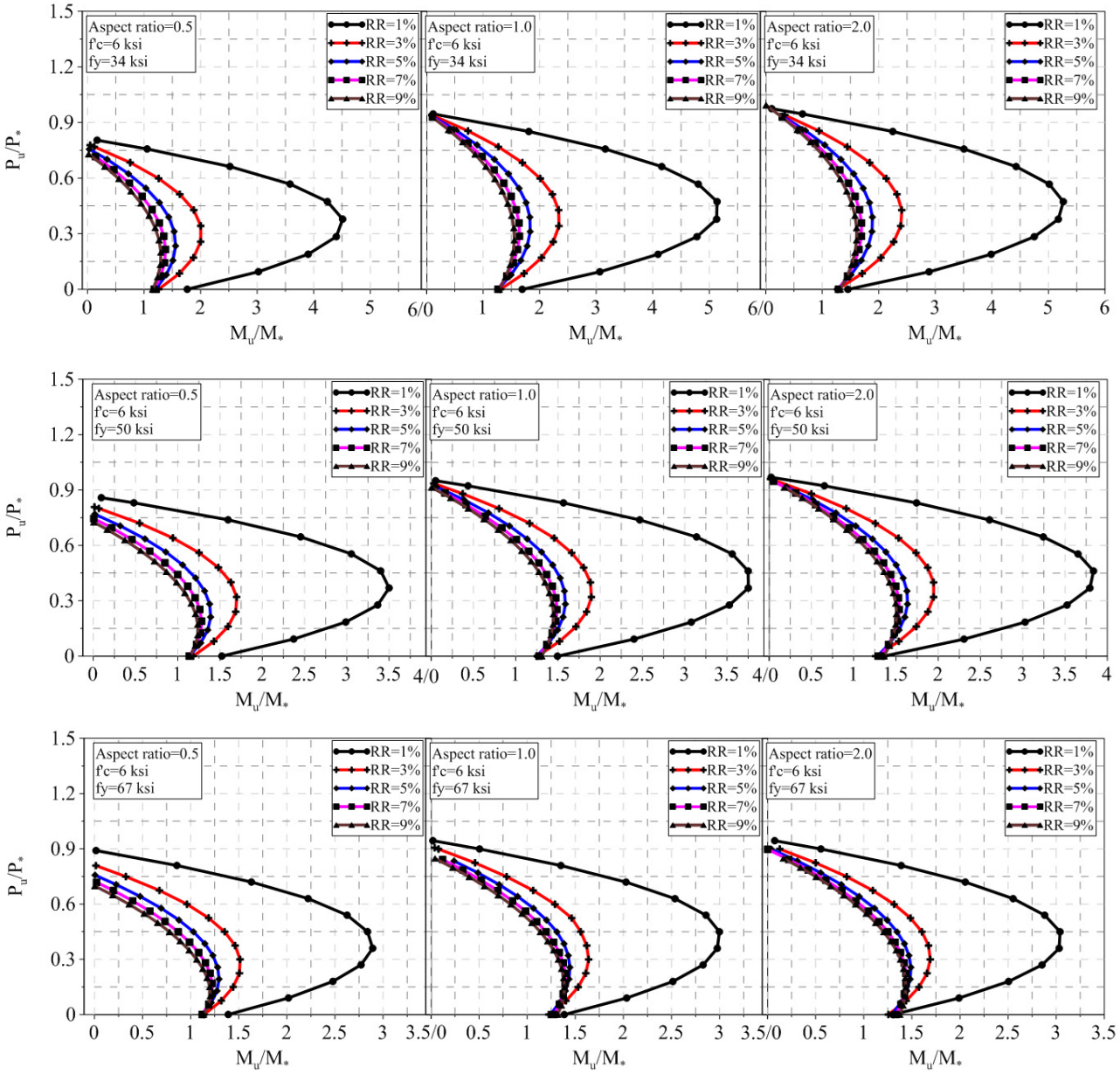

Fig. 5 – P-M interaction curves for SC wall piers (cont.)

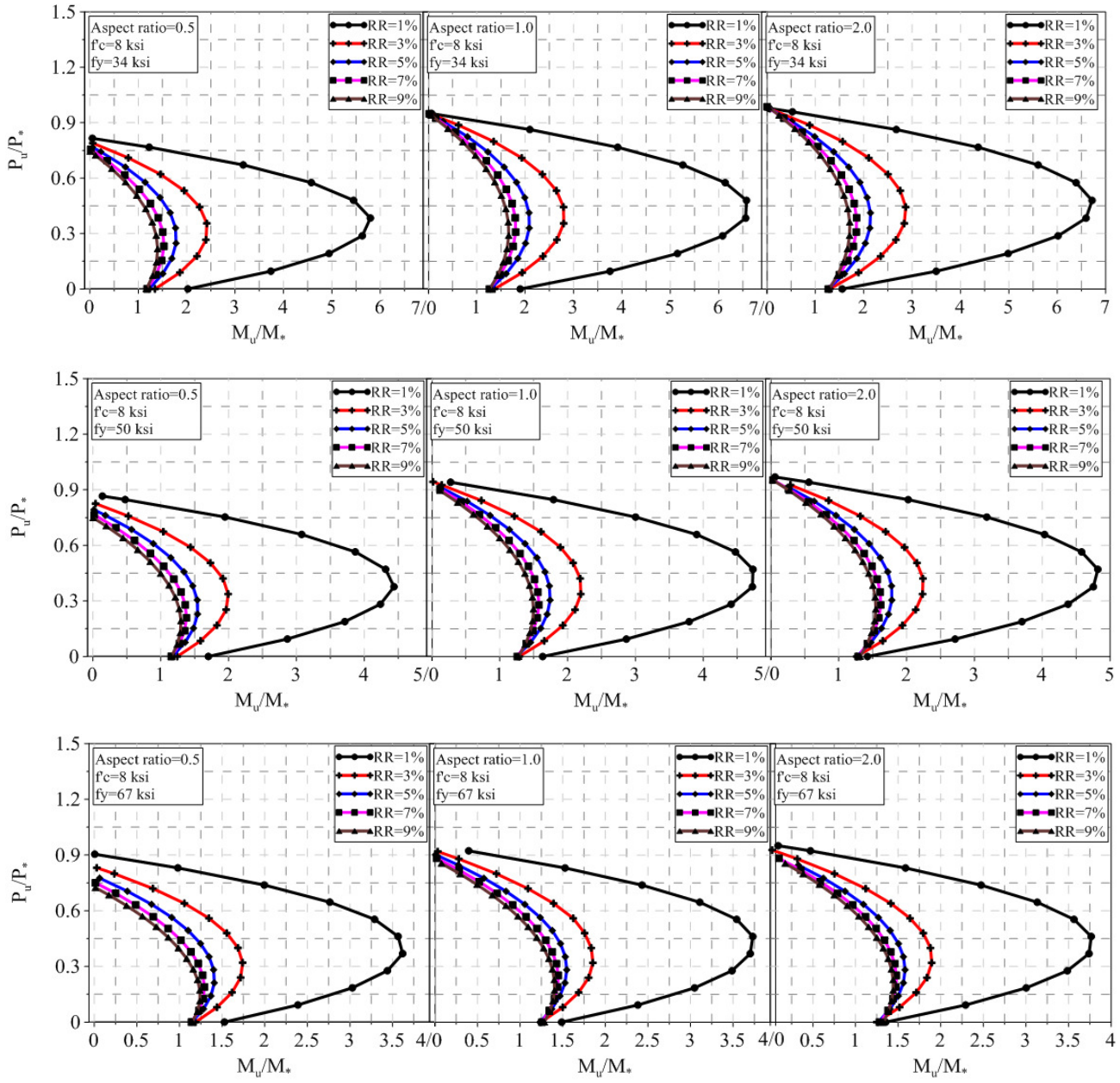

Fig. 5 – P-M interaction curves for SC wall piers (cont.)